Immunity, Volume *57*

Supplemental information

An atlas of cells in the human tonsil

Ramon Massoni-Badosa, Sergio Aguilar-Fernández, Juan C. Nieto, Paula Soler-Vila, Marc Elosua-Bayes, Domenica Marchese, Marta Kulis, Amaia Vilas-Zornoza, Marco Matteo Bühler, Sonal Rashmi, Clara Alsinet, Ginevra Caratù, Catia Moutinho, Sara Ruiz, Patricia Lorden, Giulia Lunazzi, Dolors Colomer, Gerard Frigola, Will Blevins, Lucia Romero-Rivero, Víctor Jiménez-Martínez, Anna Vidal, Judith Mateos-Jaimez, Alba Maiques-Diaz, Sara Ovejero, Jérôme Moreaux, Sara Palomino, David Gomez-Cabrero, Xabier Agirre, Marc A. Weniger, Hamish W. King, Lucy C. Garner, Federico Marini, Francisco Javier Cervera-Paz, Peter M. Baptista, Isabel Vilaseca, Cecilia Rosales, Silvia Ruiz-Gaspà, Benjamin Talks, Keval Sidhpura, Anna Pascual-Reguant, Anja E. Hauser, Muzlifah Haniffa, Felipe Prosper, Ralf Küppers, Ivo Glynne Gut, Elias Campo, José Ignacio Martin-Subero, and Holger Heyn

Supplementary Figures

Supplementary Figure Legends (S1-S7)

Supplementary Figures (S1-S7)

Figure S1. A single-cell multiomic atlas of human tonsillar cells. ***Related to Figure 1.*** (**A,G**) UMAP projection of unintegrated (*left*) and harmony-based integrated single-cell datasets (*right*) splitted and colored by data modality [scRNA-seq and multiome (A), scATAC-seq and multiome (G) and external dataset (King *et al.* (A)] (**B, H**) Boxplot comparing local inverse Simpson's Index (LISI) across confounders of integrated and unintegrated scRNA-seq (B) and scATAC-seq (H) datasets. (**C**) UMAP projection of the King *et al.* dataset colored by the original publication. **(D)** UMAP projection of the tonsillar cells of the discovery cohort colored by the main 9 cellular compartments identified: Naive and Memory B cells (NBC_MBC), Germinal center B cells (GCBC), plasma cells (PC), CD4 T cells, cytotoxic (CD8 T cells, NK, ILC, double negative T cells (DN), myeloid cells (DC, macrophages, monocytes, granulocytes, mast cells), follicular dendritic cells (FDC), epithelial cells and plasmacytoid dendritic cells (PDC). **(E)** UMAP projection of tonsillar cells colored by cell cycle phase; *left*: S Score and *right*: G2M Score. **(F)** Pie chart representing the distribution of preB and preT cells across donors. For each donor, the number and percentage of cells (out of the total preB and of the total preT) is indicated. (M: male; F: female). **(I)** UMAP projection of the prediction score inferred for CITE-seq (*left*) and scATAC-seq (*right*) after the label and coordinate transfer.

Figure S2. CD4 T follicular and non-follicular cell fate decision in the human tonsil. ***Related to Figure 2.*** (**A**) Dotplot showing the average expression of markers for Naive, CM pre-non-Tfh and CM Pre Tfh. Dot size reflects the percentage of cells in a cluster expressing each gene and the color the average expression level. (**B**) UMAP projection colored by PRDM1 and BCL6 gene expression and TF-activity gen- (red) and region (green) based obtained with SCENIC+ (STAR methods). (**C**) Dotplot showing the average expression (color) and percentage of cells expressing (size) each of the top 20 markers that described the main CD4 T subpopulations identified. **(D)** Boxplots of BCL6 accessibility values considering the gene body and 2,000 bp upstream (*top*) and the predicted distal cis-regulatoy region using Cicero as a potential enhancer (*bottom*). **(E)** Genomic snapshot of accessibility at BCL6 and distal enhancer locus across T cell clusters from KIng *et al.* **(F)** Violinplot of CD28 (*left*) and CD29 (*right*) protein expression across CD4 T cell subsets. **(G)** UMAPs projection colored by the estimated Nebulosa density expression (STAR Methods) for key interleukin and chemokine receptors. **(H)** Violinplot showing the effector Treg (eTreg, *top*) and circulating Tfr (cTfr, *bottom*) gene expression signatures from Wing JB, *et al.* computed using UCell R package for Treg subtypes.

Figure S3. Landscape of CD8 and innate lymphoid cells in the human tonsil. ***Related to Figure 3.*** (**A**) Heatmap showing the average expression of the top markers for CD8 T cells and innate lymphoid cells (ILC). **(B)** Violinplot showing the protein expression of seven representative markers for different subpopulations in CD8 T and ILC. **(C)** Violinplot showing the motif activity of TBX21 across the different subpopulations in CD8 T and ILC. **(D-G)** Immunofluorescence overlays of markers acquired by multiplex histology in one tissue section from a representative tonsil. Each image depicts the same field of view (FOV) of 665 x 665 µm, sequentially stained with the depicted fluorescence-labelled antibodies. Images contain 2048 x 2048 pixels and are generated using an inverted wide-field fluorescence microscope with a 20x objective, a lateral resolution of 325 nm and an axial resolution above 5 µm. The thin dotted line represents the B cell follicle and the thick dotted line represents the epithelial layer. **(D)** CD20 (cyan) depicts the B cell follicle, CD3 (yellow) marks the T cell zone and pancytokeratin (PCK; magenta) stains the epithelium**. (E)** The endothelial marker CD34 (green) and the myofibroblast marker smooth muscle actin (SMA; red) depict the vessels, and vimentin (blue) marks the fibroblast-dense areas. **(F)** Granzyme A (GzmA; magenta), Eomes (yellow) and CD8 (magenta) represent cytotoxic T cells. **(G)** CD49a (cyan), CD69 (magenta) and CD103 (yellow) mark tissue resident cells. **(C-D)** White outlined squares represent areas of interest, shown as enlargements and single channel images. RM CD8 T cells (CD103+CD69+CD49a+/-) are shown as white arrows and are preferentially localized within the epithelium and in the connective tissue septum lining the tonsillar crypts, but not within the B cell follicles and rarely deep within the T cell zone. (**H**) UMAP projection of CD4 T, CD8 T, NK, ILC and DN in the CITE-seq dataset. (**I**) Protein expression of CD3, CD4 and CD8 across major lymphocyte populations (CITE-seq dataset). (**J**) In silico gating of major lymphocyte populations based on CD4 and CD8 protein expression. (**K**) Distribution of gated groups across each major population. (**L**) FACS validation of DN T cells in tonsils.

Figure S4. B cell activation and GC dynamics. ***Related to Figure 4.*** (**A**) Dotplot showing marker expression for NBC and MBC subpopulations. (**B**) Dotplot showing marker expression per GCBC subpopulations. Dot size reflects the percentage of cells in a cluster expressing each gene and the color the average expression level. (**C, D**) UMAP projection of GCBC cells colored by cell cycle phase (C) or GCBC annotation (D) and splitted by cell cycle correction strategy. (**E**) Local inverse Simpson's Index (LISI) for both annotation [top, related with (D)] and cell cycle phase [bottom, related with (E)]. (**F**) UMAP projection of NFKB signature computed using *UCell* R package with seven genes (*NFKBIA*, *NFKBID*, *NFKB1*, *NFKB2*, *REL*, *RELA*, *RELB*) for NBC and MBC. (**G**) UMAP projection of *BATF* expression in NBC and MBC.

Figure S5. Plasma cell differentiation and cell identity regulation in human tonsils. ***Related to Figure 5.*** (**A**) PC BCR analysis. Top: CITE-seq/BCR cells projected in scRNA-seq UMAP coordinates. Cluster labels and coordinates are transferred via KNN classification and regression respectively. Bottom: Barplot representation of PC clonality. Blue, clonal expansion when >= 3 cells had identical CDR3 sequence; Green, two cells share identical sequence; Orange, cells with distinct CDR3 sequence. (**B**) Proliferative cells (PB committed, Transitional PB, PB) differentiation analysis. Top: UMAP projection of proliferative cells colored by cell cycle phase. Bottom: Barplot representation of PC-phenotypic markers expression across S and G2M cells from PB cluster (most representative proliferative cluster). (**C**) UMAPs projection of the expression of Ig and MBC genes (BANK1, CELF2, TXNIP). (**D**) Violin Plot of the Endoplasmic Reticulum (ER) signature across PC scRNA-seq clusters. Signature was obtained using the *UCell* R package with 70 genes obtained from the DAVID KEGG pathway analysis: Protein processing in endoplasmic reticulum. (**E**) Cell type proportions deconvoluted using SPOTlight (see Methods). (**F**) Spatially defined trajectories on H&E stained images from BCLL-10-T (left) and BCLL-12-T (right) patients and heatmap showing smoothed expression changes for specific genes across defined trajectories. BCLL-10-T trajectory starts in a LZ zone and includes an interfollicular zone. (**G**) Correlation plot showing co-localization of cell types on the Visium slides, plot for slide BCLL-10-T (top) and for all slides combined (bottom). (**H**) UMAP projection of the activity (AUCell score) of VDR and CREB3 TFs. (**I**) Barplot of SIX5 expression in different subpopulations from peripheral blood scRNA-seq data from Hao Yuhan *et al.*. (**J**) Boxplot of PC phenotypic markers, SIX5 and SIX5 predicted target in different populations from bone marrow scRNA-seq data from Hay Stuart B *et al.*. Link http://www.altanalyze.org/ICGS/HCA/Viewer.php

Figure S6. Epithelial cells in the human tonsils. ***Related to Figure 6.*** (**A**) UMAP projection of epithelial tonsillar cells colored and numbered by scRNA-seq clusters. (**B**) Dotplot showing the average expression of the top markers that described the main clusters identified in the epithelial compartment. Dot size reflects the percentage of cells in a cluster expressing each gene and the color the average expression level. **(C)** Cell type proportions of populations of interest within each spot on slide BCLL-2-T along with an H&E image of the tissue slice. Cell type deconvolution was carried out with SPOTlight. We deconvoluted the spots using epithelial cell subpopulation annotations along with the general annotation of other cell types ensuring we captured the biological signal of all our cell types. (**D**) UMAP projection of follicular dendritic cells (FDC) and other cells from mesenchymal origin colored and numbered by scRNA-seq clusters. (**E**) Dotplot showing the average expression of the top markers that described the main clusters identified. **(F)** MAGIC-normalized gene expression of genes of interest on slide BCLL-10-T. (**G**) Dotplot showing the average expression of the top markers that described the main clusters identified in the DC (*left*) and aDC (*right*) compartment. Dot size reflects the percentage of cells in a cluster expressing each gene and the color the average expression level. **(H)** Boxplot showing the proliferation signatures (S.Score and G2M.Score) for DC1 precursor and DC1 mature cells. **(I)** Violinplot showing seven signatures computed using UCell R package for aDC subsets. **(J)** Stacked barplot showing the proportion of cells *(y-axis*) detected in each donor (*x-axis*) for each subpopulation. **(K)** Dotplot showing the average expression of three markers (C1QA, MMP12, SELENOP) across all defined cell types and states in the tonsil atlas.

Figure S7. Confirmation of presence, annotation and markers of tonsillar cell types using a validation cohort and Analysis of two MCL samples in the light of the tonsil atlas. ***Related to Figure 7.*** (**A**, **C**, **E**, **G; I**) UMAP projection of reference (left, discovery cohort) and query (right, validation cohort) for naive and memory B cells [NBC/MBC, (A)], germinal center B cells [GCBC, (C)], plasma cells [PC, (E)], CD8 T (G) and myeloid cells (I). (**B**, **D**, **F**, **H, J**) Heatmap showing scaled mean marker expression for NBC/MBC (B), GCBC (D), PC (F), CD8 T (H) and myeloid cells (J). Boxplots represent the annotation confidence for each cluster. (**K**) UMAP projection the expression of six genes encoded in chromosome Y for M102 (top) and M413 (bottom). (**L**) Distribution and UMAP projection of a chrY expression signature derived from the six genes shown in (A) for M102 (left) and M413 (right). Vertical dashed line shows the cutoff used to classify cells in chrY+/-. (**M**) UMAP projection of the annotated clusters for M413. (**N**) Dotplot showing the average expression (color) and percentage of expressing cells (size) of the top markers that described the main clusters identified in for M413. (**O**, **P**) Heatmaps showing the copy number alterations (CNA) inferred from transcriptomics data with infercnv for M102 (O) and M413 (P).

Figure S1

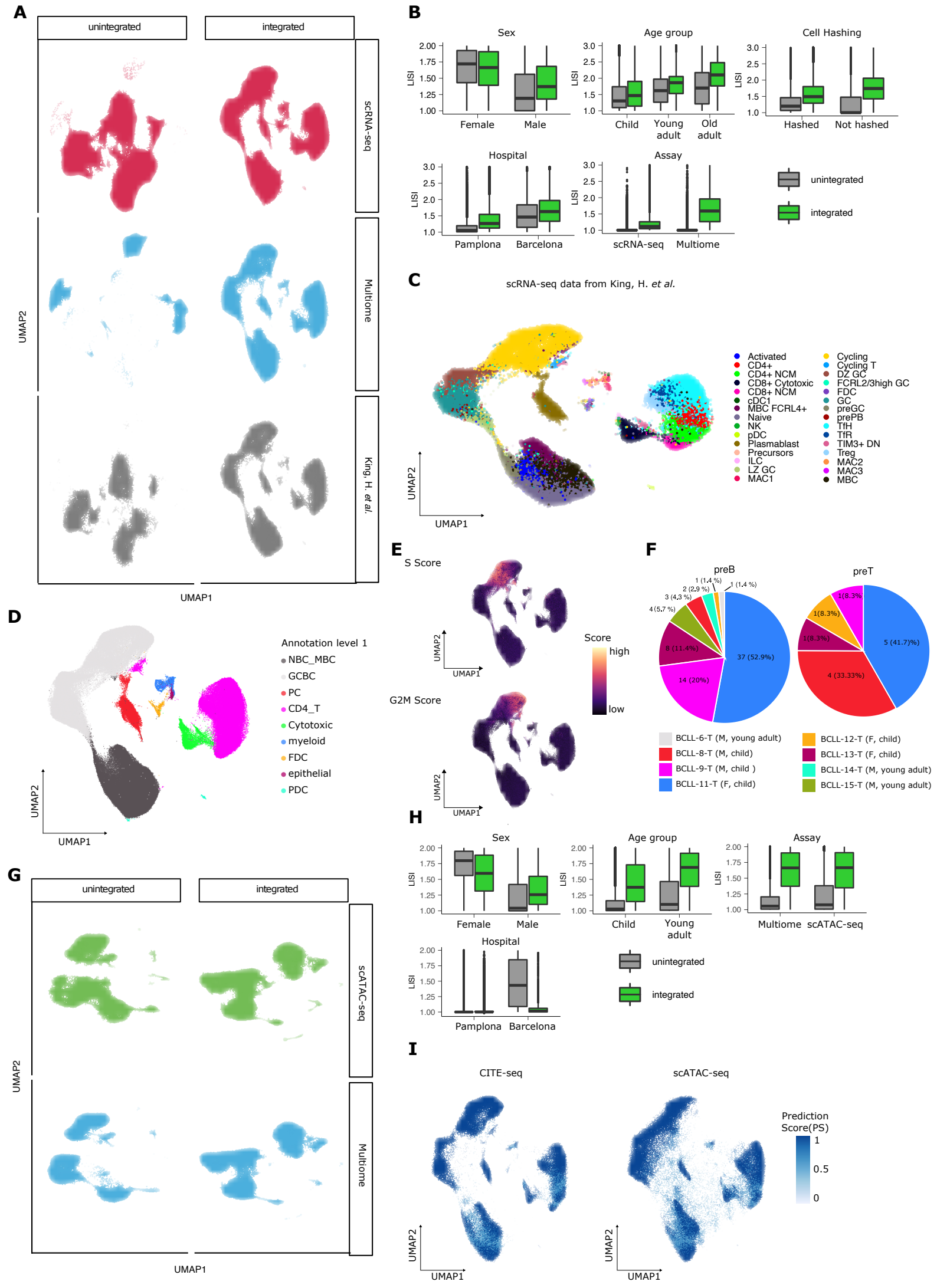
A
unintegrated
integrated
scRNA-seq
Multiome
King, H. et al.
UMAP2
UMAP1
B
Sex
Age group
Cell Hashing
Hospital
Assay
LISI
Female
Male
Child
Young adult
Old adult
Hashed
Not hashed
Pamplona
Barcelona
scRNA-seq
Multiome
unintegrated
integrated
C
scRNA-seq data from King, H. et al.
Activated
CD4+
CD4+ NCM
CD8+ Cytotoxic
CD8+ NCM
cDC1
MBC FCRL4+
Naive
NK
pDC
Plasmablast
Precursors
ILC
LZ GC
MAC1
Cycling
Cycling T
DZ GC
FCRL2/3high GC
FDC
GC
preGC
prePB
TfH
TfR
TIM3+ DN
Treg
MAC2
MAC3
MBC
D
Annotation level 1
NBC_MBC
GCBC
PC
CD4_T
Cytotoxic
myeloid
FDC
epithelial
PDC
E
S Score
G2M Score
Score
high
low
F
preB
preT
37 (52.9%)
14 (20%)
8 (11.4%)
4(5.7 %)
3 (4.3 %)
2 (2.9 %)
1 (1.4 %)
5 (41.7)%)
4 (33.33%)
1(8.3%)
BCLL-6-T (M, young adult)
BCLL-8-T (M, child)
BCLL-9-T (M, child)
BCLL-11-T (F, child)
BCLL-12-T (F, child)
BCLL-13-T (F, child)
BCLL-14-T (M, young adult)
BCLL-15-T (M, young adult)
G
unintegrated
integrated
scATAC-seq
Multiome
H
Sex
Age group
Assay
Hospital
Female
Male
Child
Young adult
Multiome
scATAC-seq
Pamplona
Barcelona
I
CITE-seq
scATAC-seq
Prediction Score(PS)
1
0.5
0

Figure S2

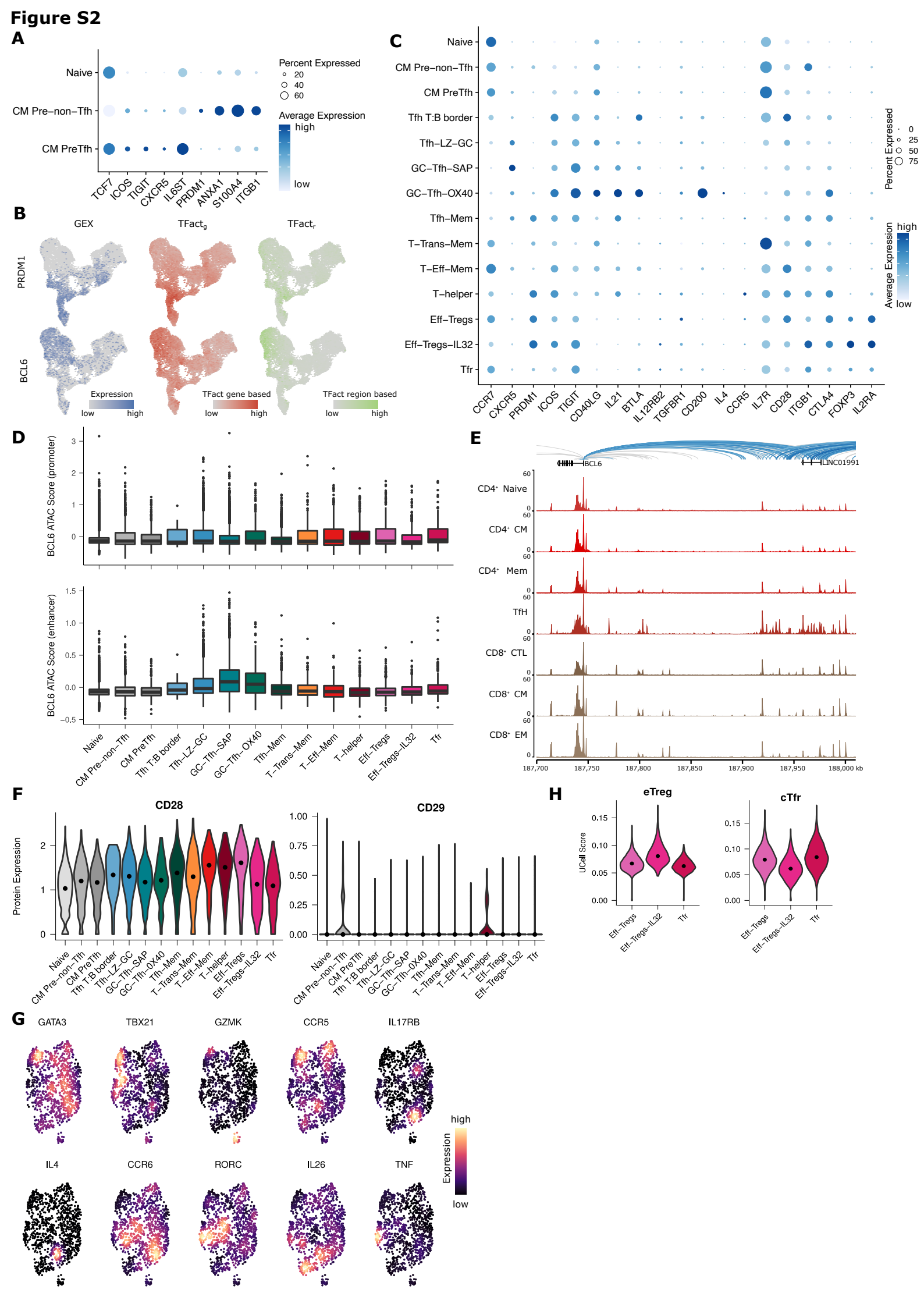
A
Naive
CM Pre−non−Tfh
CM PreTfh
TCF7
ICOS
TIGIT
CXCR5
IL6ST
PRDM1
ANXA1
S100A4
ITGB1
Percent Expressed
20
40
60
Average Expression
high
low
B
GEX
TFact$_g$
TFact$_r$
PRDM1
BCL6
Expression
low
high
TFact gene based
low
high
TFact region based
low
high
C
Naive
CM Pre−non−Tfh
CM PreTfh
Tfh T:B border
Tfh−LZ−GC
GC−Tfh−SAP
GC−Tfh−OX40
Tfh−Mem
T−Trans−Mem
T−Eff−Mem
T−helper
Eff−Tregs
Eff−Tregs−IL32
Tfr
CCR7
CXCR5
PRDM1
ICOS
TIGIT
CD40LG
IL21
BTLA
IL12RB2
TGFBR1
CD200
IL4
CCR5
IL7R
CD28
ITGB1
CTLA4
FOXP3
IL2RA
Percent Expressed
0
25
50
75
Average Expression
high
low
D
BCL6 ATAC Score (promoter)
BCL6 ATAC Score (enhancer)
Naive
CM Pre−non−Tfh
CM PreTfh
Tfh T:B border
Tfh−LZ−GC
GC−Tfh−SAP
GC−Tfh−OX40
Tfh−Mem
T−Trans−Mem
T−Eff−Mem
T−helper
Eff−Tregs
Eff−Tregs−IL32
Tfr
E
BCL6
LINC01991
CD4⁺ Naive
CD4⁺ CM
CD4⁺ Mem
TfH
CD8⁺ CTL
CD8⁺ CM
CD8⁺ EM
187,700
187,750
187,800
187,850
187,900
187,950
188,000 kb
F
CD28
CD29
Protein Expression
Naive
CM Pre−non−Tfh
CM PreTfh
Tfh T:B border
Tfh−LZ−GC
GC−Tfh−SAP
GC−Tfh−OX40
Tfh−Mem
T−Trans−Mem
T−Eff−Mem
T−helper
Eff−Tregs
Eff−Tregs−IL32
Tfr
H
eTreg
cTfr
UCell Score
Eff−Tregs
Eff−Tregs−IL32
Tfr
G
GATA3
TBX21
GZMK
CCR5
IL17RB
IL4
CCR6
RORC
IL26
TNF
high
Expression
low

Figure S3

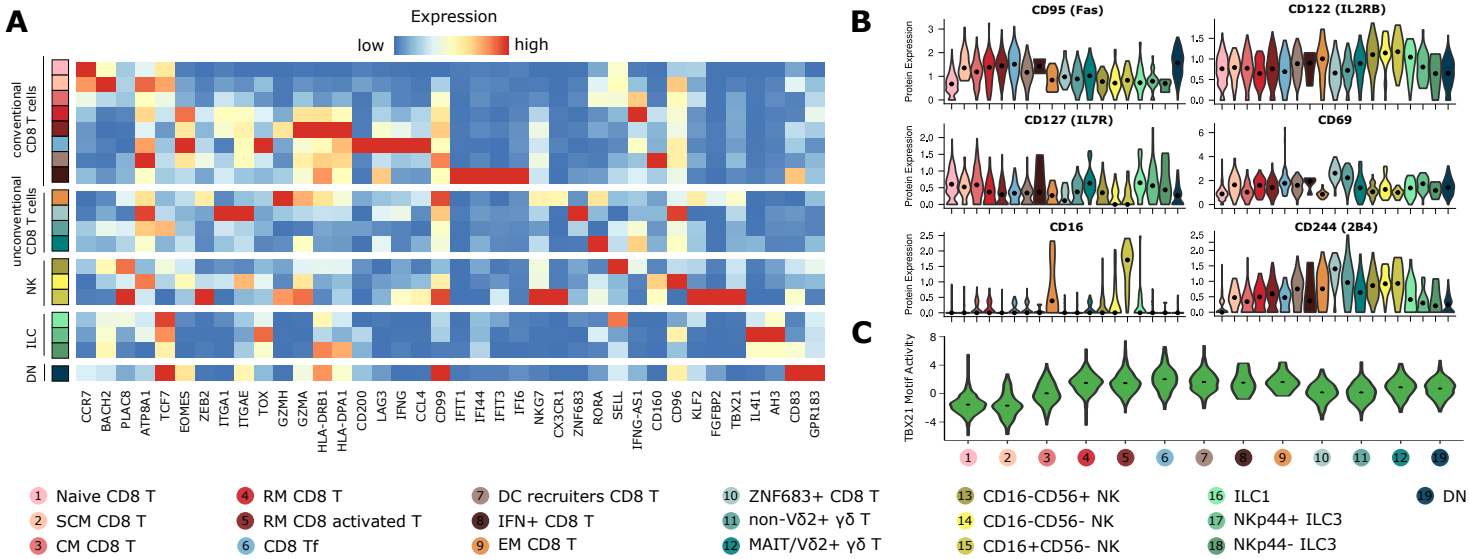
A
Expression
low
high
conventional CD8 T cells
unconventional CD8 T cells
NK
ILC
DN
CCR7 BACH2 PLAC8 ATP8A1 TCF7 EOMES ZEB2 ITGA1 ITGAE TOX GZMH GZMA HLA-DRB1 HLA-DPA1 CD200 LAG3 IFNG CCL4 CD99 IFIT1 IFI44 IFIT3 IFI6 NKG7 CX3CR1 ZNF683 RORA SELL IFNG-AS1 CD160 CD96 KLF2 FGFBP2 TBX21 IL4I1 AH3 CD83 GPR183
B
CD95 (Fas)
CD122 (IL2RB)
CD127 (IL7R)
CD69
CD16
CD244 (2B4)
Protein Expression
C
TBX21 Motif Activity
1 Naive CD8 T
2 SCM CD8 T
3 CM CD8 T
4 RM CD8 T
5 RM CD8 activated T
6 CD8 Tf
7 DC recruiters CD8 T
8 IFN+ CD8 T
9 EM CD8 T
10 ZNF683+ CD8 T
11 non-Vδ2+ γδ T
12 MAIT/Vδ2+ γδ T
13 CD16-CD56+ NK
14 CD16-CD56- NK
15 CD16+CD56- NK
16 ILC1
17 NKp44+ ILC3
18 NKp44- ILC3
19 DN

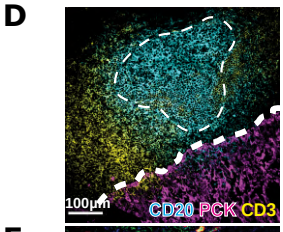
D
100µm
CD20 PCK CD3

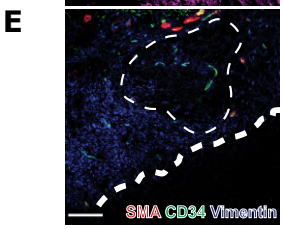
E
SMA CD34 Vimentin

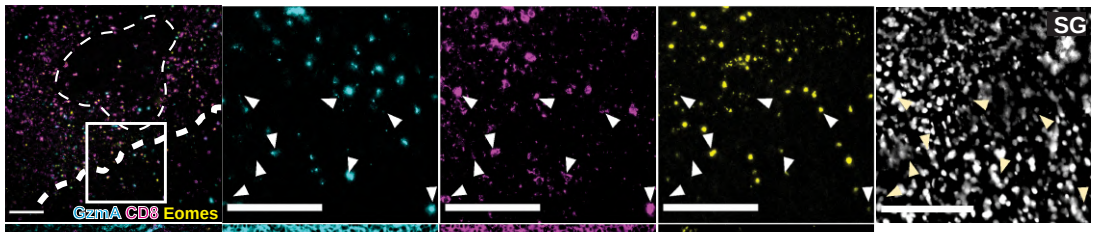
F
GzmA CD8 Eomes
SG

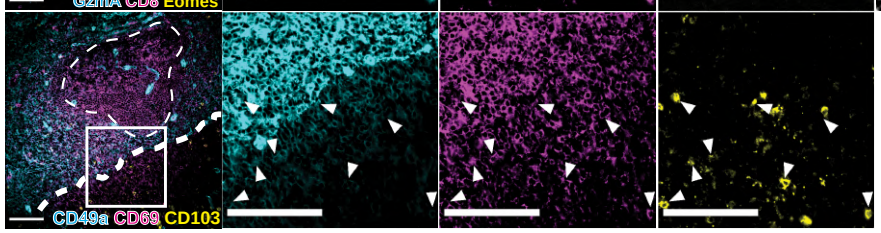
G
CD49a CD69 CD103

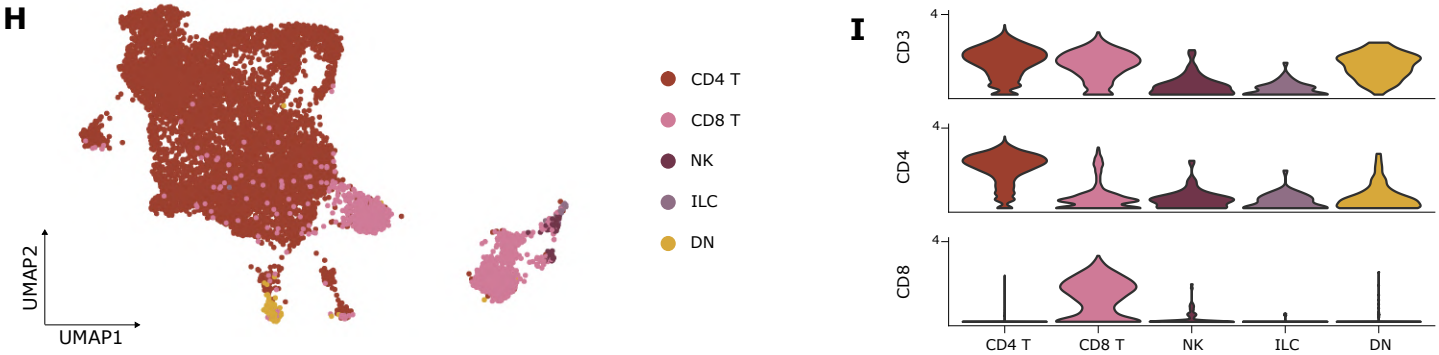
H
UMAP2
UMAP1
CD4 T
CD8 T
NK
ILC
DN
I
CD3
CD4
CD8
CD4 T
CD8 T
NK
ILC
DN

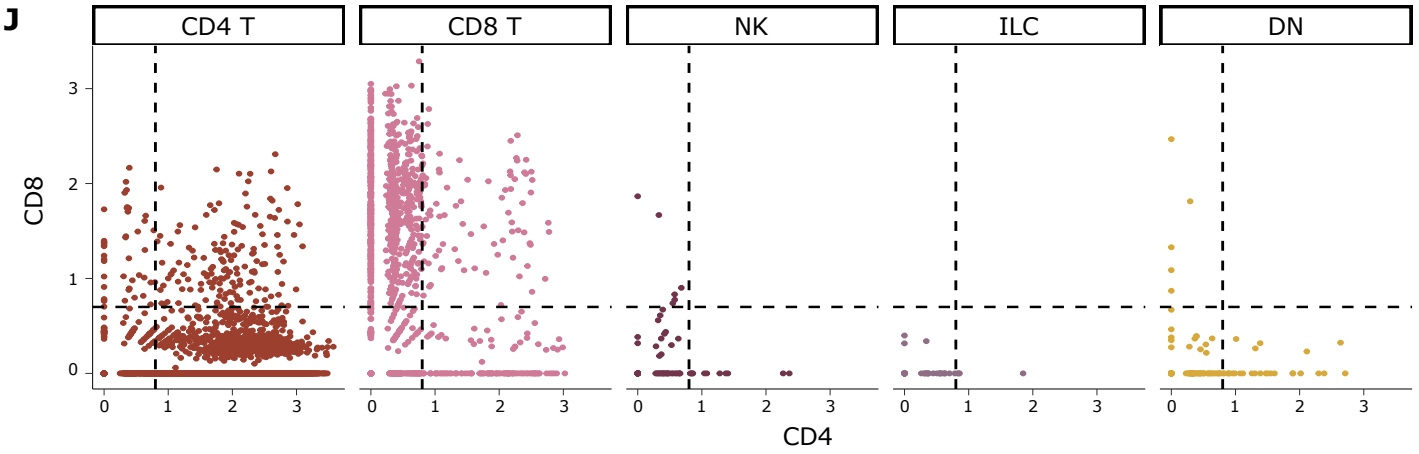
J
CD4 T
CD8 T
NK
ILC
DN
CD8
CD4

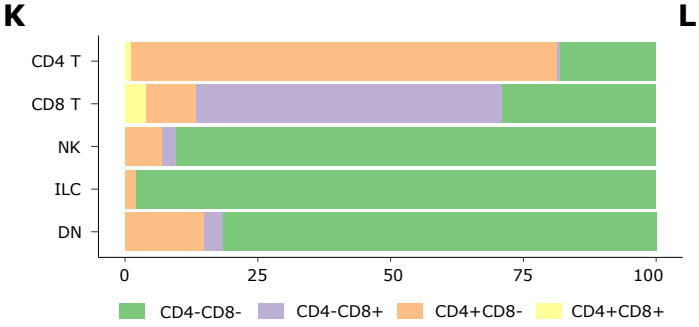
K
CD4 T
CD8 T
NK
ILC
DN
CD4-CD8-
CD4-CD8+
CD4+CD8-
CD4+CD8+

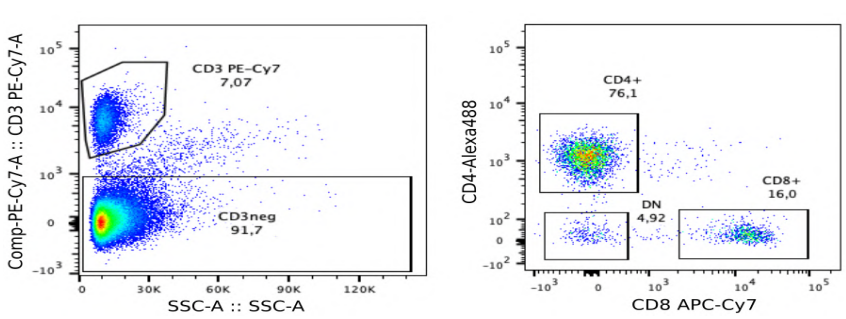
L
CD3 PE-Cy7
7,07
CD3neg
91,7
Comp-PE-Cy7-A :: CD3 PE-Cy7-A
SSC-A :: SSC-A
CD4+
76,1
CD8+
16,0
DN
4,92
CD4-Alexa488
CD8 APC-Cy7

Figure S4

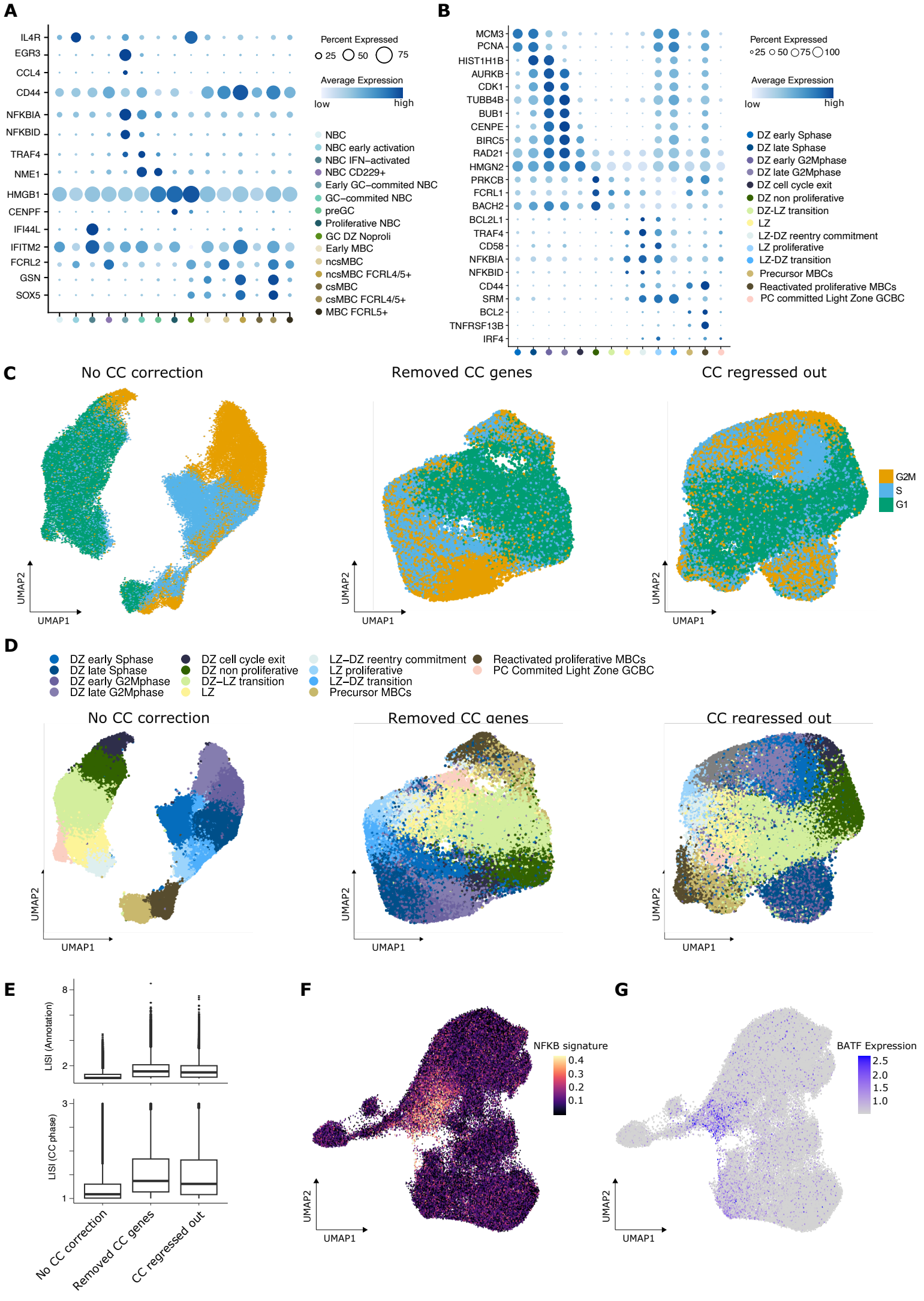
A
IL4R
EGR3
CCL4
CD44
NFKBIA
NFKBID
TRAF4
NME1
HMGB1
CENPF
IFI44L
IFITM2
FCRL2
GSN
SOX5
Percent Expressed
25 50 75
Average Expression
low high
NBC
NBC early activation
NBC IFN–activated
NBC CD229+
Early GC–commited NBC
GC–commited NBC
preGC
Proliferative NBC
GC DZ Noproli
Early MBC
ncsMBC
ncsMBC FCRL4/5+
csMBC
csMBC FCRL4/5+
MBC FCRL5+
B
MCM3
PCNA
HIST1H1B
AURKB
CDK1
TUBB4B
BUB1
CENPE
BIRC5
RAD21
HMGN2
PRKCB
FCRL1
BACH2
BCL2L1
TRAF4
CD58
NFKBIA
NFKBID
CD44
SRM
BCL2
TNFRSF13B
IRF4
Percent Expressed
25 50 75 100
Average Expression
low high
DZ early Sphase
DZ late Sphase
DZ early G2Mphase
DZ late G2Mphase
DZ cell cycle exit
DZ non proliferative
DZ-LZ transition
LZ
LZ-DZ reentry commitment
LZ proliferative
LZ-DZ transition
Precursor MBCs
Reactivated proliferative MBCs
PC committed Light Zone GCBC
C
No CC correction
Removed CC genes
CC regressed out
G2M
S
G1
UMAP2
UMAP1
D
DZ early Sphase
DZ late Sphase
DZ early G2Mphase
DZ late G2Mphase
DZ cell cycle exit
DZ non proliferative
DZ–LZ transition
LZ
LZ–DZ reentry commitment
LZ proliferative
LZ–DZ transition
Precursor MBCs
Reactivated proliferative MBCs
PC Commited Light Zone GCBC
No CC correction
Removed CC genes
CC regressed out
UMAP2
UMAP1
E
LISI (Annotation)
LISI (CC phase)
No CC correction
Removed CC genes
CC regressed out
F
NFKB signature
0.4
0.3
0.2
0.1
UMAP2
UMAP1
G
BATF Expression
2.5
2.0
1.5
1.0
UMAP2
UMAP1

Figure S5

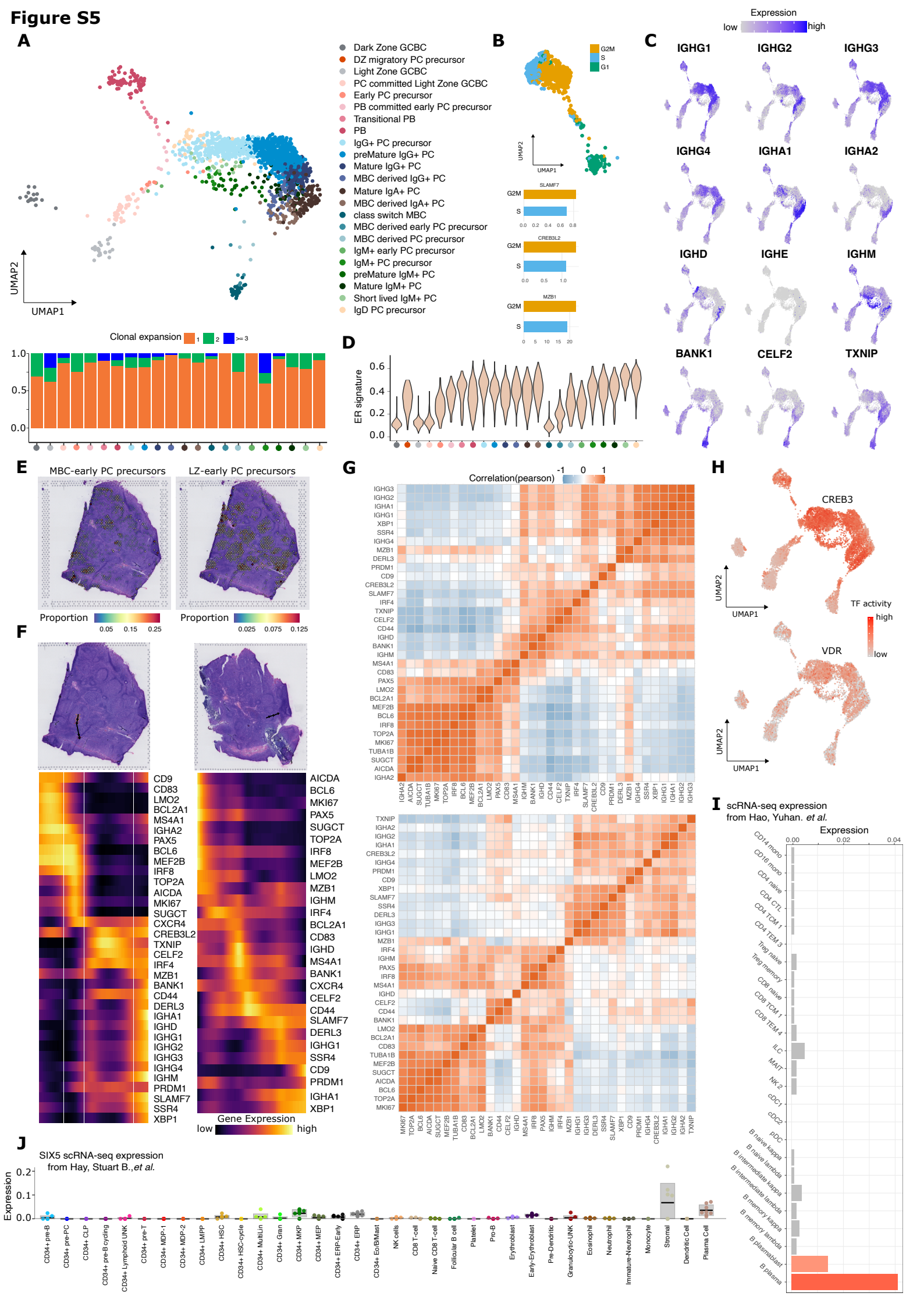
A
Dark Zone GCBC
DZ migratory PC precursor
Light Zone GCBC
PC committed Light Zone GCBC
Early PC precursor
PB committed early PC precursor
Transitional PB
PB
IgG+ PC precursor
preMature IgG+ PC
Mature IgG+ PC
MBC derived IgG+ PC
Mature IgA+ PC
MBC derived IgA+ PC
class switch MBC
MBC derived early PC precursor
MBC derived PC precursor
IgM+ early PC precursor
IgM+ PC precursor
preMature IgM+ PC
Mature IgM+ PC
Short lived IgM+ PC
IgD PC precursor
UMAP2
UMAP1
Clonal expansion 1 2 >= 3
B
G2M
S
G1
SLAMF7
CREB3L2
MZB1
C
Expression
low high
IGHG1
IGHG2
IGHG3
IGHG4
IGHA1
IGHA2
IGHD
IGHE
IGHM
BANK1
CELF2
TXNIP
D
ER signature
E
MBC-early PC precursors
LZ-early PC precursors
Proportion
F
Gene Expression
low high
G
Correlation(pearson)
H
CREB3
VDR
TF activity
high
low
I
scRNA-seq expression
from Hao, Yuhan. et al.
Expression
J
SIX5 scRNA-seq expression
from Hay, Stuart B.,et al.
Expression

Figure S6

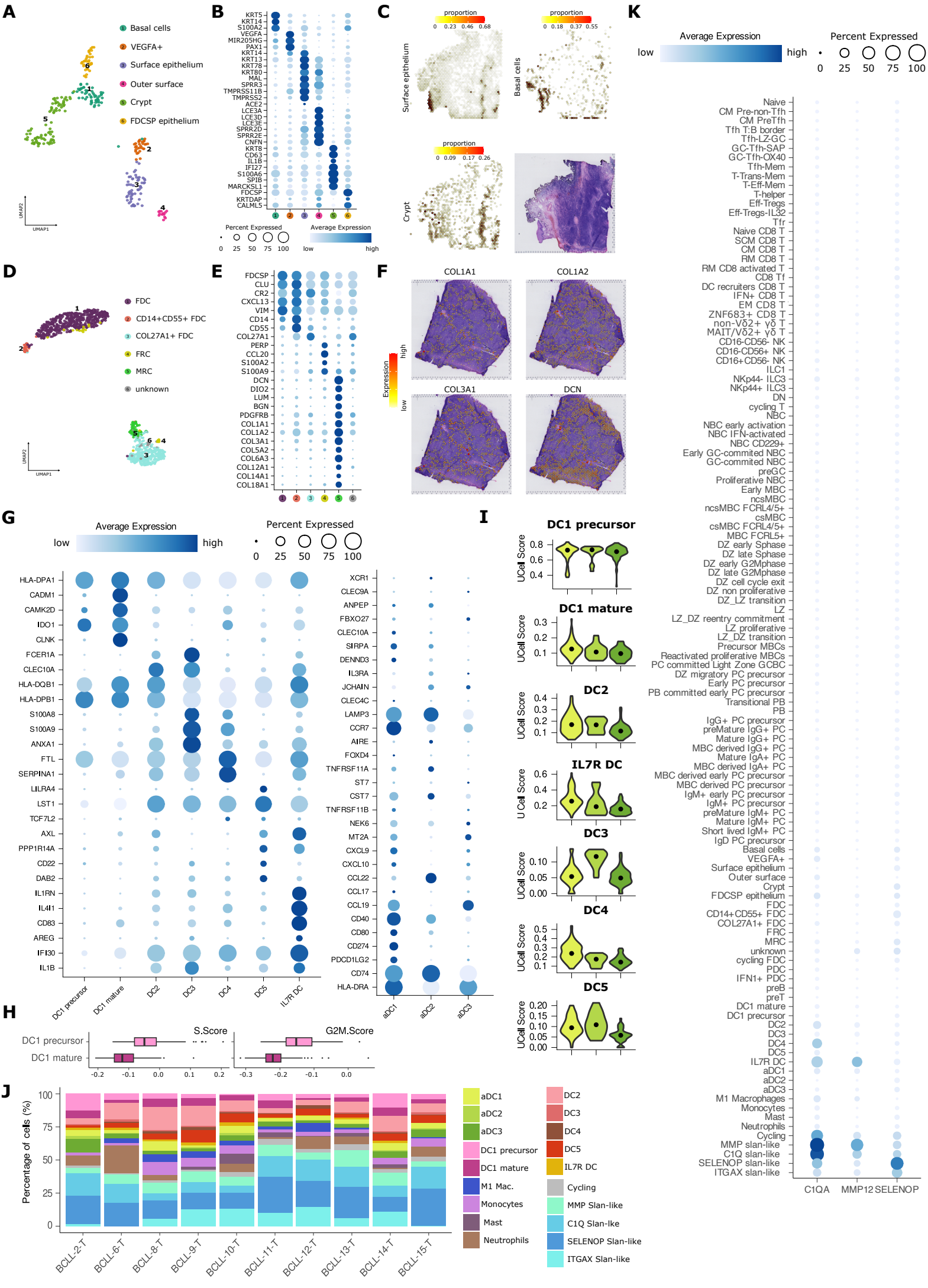
A
Basal cells
VEGFA+
Surface epithelium
Outer surface
Crypt
FDCSP epithelium
B
Percent Expressed
Average Expression
low
high
C
proportion
Surface epithelium
Basal cells
Crypt
D
FDC
CD14+CD55+ FDC
COL27A1+ FDC
FRC
MRC
unknown
E
F
COL1A1
COL1A2
COL3A1
DCN
Expression
G
Average Expression
Percent Expressed
DC1 precursor
DC1 mature
DC2
DC3
DC4
DC5
IL7R DC
aDC1
aDC2
aDC3
H
S.Score
G2M.Score
I
DC1 precursor
DC1 mature
DC2
IL7R DC
DC3
DC4
DC5
UCell Score
J
Percentage of cells (%)
BCLL-2-T
BCLL-6-T
BCLL-8-T
BCLL-9-T
BCLL-10-T
BCLL-11-T
BCLL-12-T
BCLL-13-T
BCLL-14-T
BCLL-15-T
aDC1
aDC2
aDC3
DC1 precursor
DC1 mature
M1 Mac.
Monocytes
Mast
Neutrophils
DC2
DC3
DC4
DC5
IL7R DC
Cycling
MMP Slan-like
C1Q Slan-lke
SELENOP Slan-like
ITGAX Slan-like
K
Average Expression
Percent Expressed
C1QA
MMP12
SELENOP

Figure S7

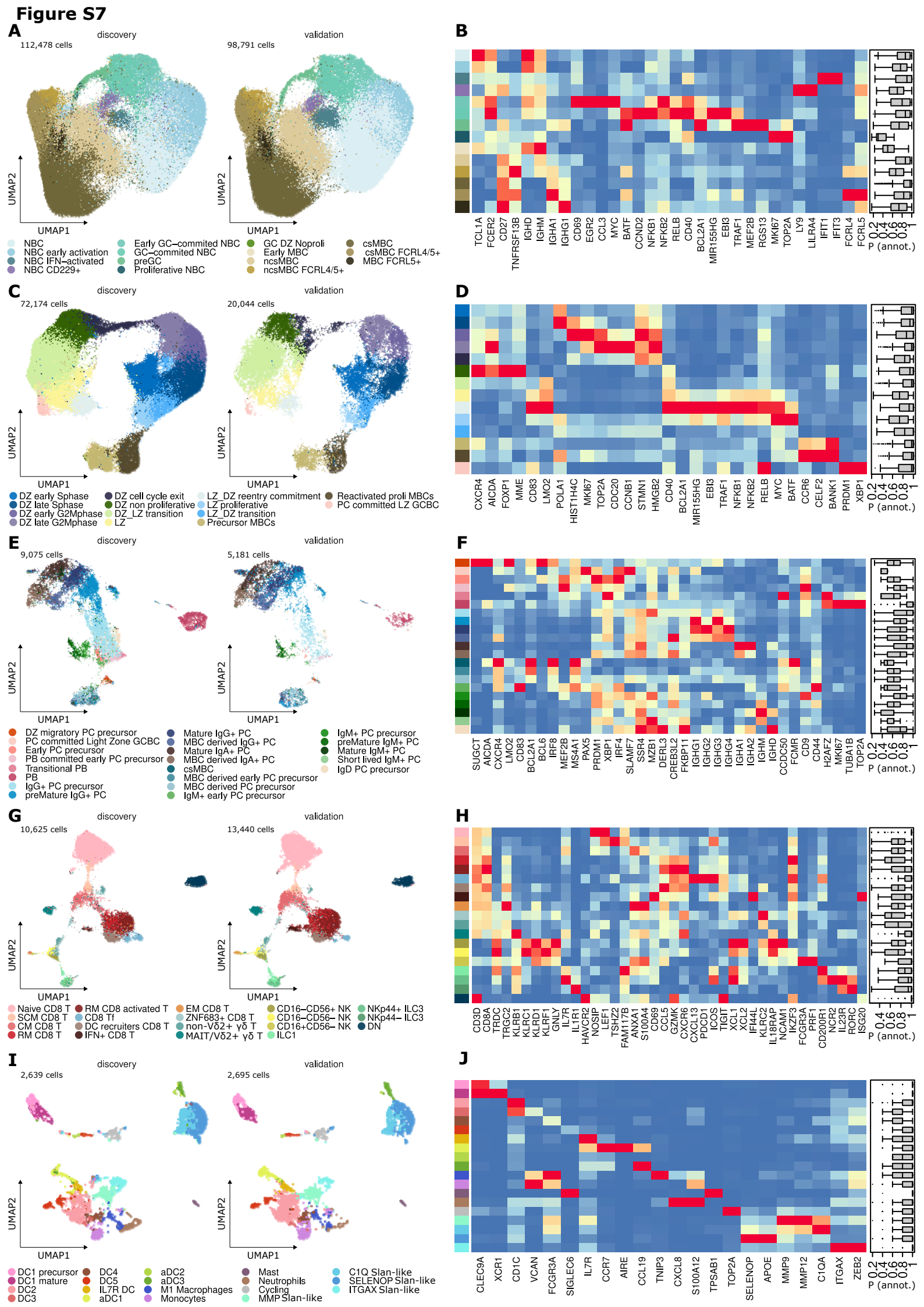
A
discovery
validation
112,478 cells
98,791 cells
UMAP1
UMAP2
NBC
NBC early activation
NBC IFN–activated
NBC CD229+
Early GC–commited NBC
GC–commited NBC
preGC
Proliferative NBC
GC DZ Noproli
Early MBC
ncsMBC
ncsMBC FCRL4/5+
csMBC
csMBC FCRL4/5+
MBC FCRL5+
B
TCL1A FCER2 CD27 TNFRSF13B IGHD IGHM IGHA1 IGHG1 CD69 EGR2 CCL3 MYC BATF CCND2 NFKB1 NFKB2 RELB CD40 BCL2A1 MIR155HG EBI3 TRAF1 MEF2B RGS13 MKI67 TOP2A LY9 LILRA4 IFIT1 IFIT3 FCRL4 FCRL5
P (annot.)
C
discovery
validation
72,174 cells
20,044 cells
DZ early Sphase
DZ late Sphase
DZ early G2Mphase
DZ late G2Mphase
DZ cell cycle exit
DZ non proliferative
DZ_LZ transition
LZ
LZ_DZ reentry commitment
LZ proliferative
LZ_DZ transition
Precursor MBCs
Reactivated proli MBCs
PC committed LZ GCBC
D
CXCR4 AICDA FOXP1 MME CD83 LMO2 POLA1 HIST1H4C MKI67 TOP2A CDC20 CCNB1 STMN1 HMGB2 CD40 BCL2A1 MIR155HG EBI3 TRAF1 NFKB1 NFKB2 RELB MYC BATF CCR6 CELF2 BANK1 PRDM1 XBP1
P (annot.)
E
discovery
validation
9,075 cells
5,181 cells
DZ migratory PC precursor
PC committed Light Zone GCBC
Early PC precursor
PB committed early PC precursor
Transitional PB
PB
IgG+ PC precursor
preMature IgG+ PC
Mature IgG+ PC
MBC derived IgG+ PC
Mature IgA+ PC
MBC derived IgA+ PC
csMBC
MBC derived early PC precursor
MBC derived PC precursor
IgM+ early PC precursor
IgM+ PC precursor
preMature IgM+ PC
Mature IgM+ PC
Short lived IgM+ PC
IgD PC precursor
F
SUGCT AICDA CXCR4 LMO2 CD83 BCL2A1 BCL6 IRF8 MEF2B MS4A1 PAX5 PRDM1 XBP1 IRF4 SLAMF7 SSR4 MZB1 DERL3 CREB3L2 FKBP11 IGHG1 IGHG2 IGHG3 IGHG4 IGHA1 IGHA2 IGHM IGHD CCDC50 FCMR CD9 CD44 H2AFZ MKI67 TUBA1B TOP2A
P (annot.)
G
discovery
validation
10,625 cells
13,440 cells
Naive CD8 T
SCM CD8 T
CM CD8 T
RM CD8 T
RM CD8 activated T
CD8 Tf
DC recruiters CD8 T
IFN+ CD8 T
EM CD8 T
ZNF683+ CD8 T
non-Vδ2+ γδ T
MAIT/Vδ2+ γδ T
CD16–CD56+ NK
CD16–CD56– NK
CD16+CD56– NK
ILC1
NKp44+ ILC3
NKp44– ILC3
DN
H
CD3D CD8A TRDC TRGC2 KLRB1 KLRC1 KLRD1 KLRF1 GNLY IL7R IL1R1 HAVCR2 NOSIP LEF1 TSHZ2 FAM117B ANXA1 S100A4 CD69 CCL5 GZMK CXCR6 CXCL13 PDCD1 ICOS TIGIT XCL1 XCL2 IFI44L KLRC2 IL18RAP NCAM1 IKZF3 FCGR3A PRF1 CD200R1 NCR2 IL23R RORC ISG20
P (annot.)
I
discovery
validation
2,639 cells
2,695 cells
DC1 precursor
DC1 mature
DC2
DC3
DC4
DC5
IL7R DC
aDC1
aDC2
aDC3
M1 Macrophages
Monocytes
Mast
Neutrophils
Cycling
MMP Slan-like
C1Q Slan-like
SELENOP Slan-like
ITGAX Slan-like
J
CLEC9A XCR1 CD1C VCAN FCGR3A SIGLEC6 IL7R CCR7 AIRE CCL19 TNIP3 CXCL8 S100A12 TPSAB1 TOP2A SELENOP APOE MMP9 MMP12 C1QA ITGAX ZEB2
P (annot.)

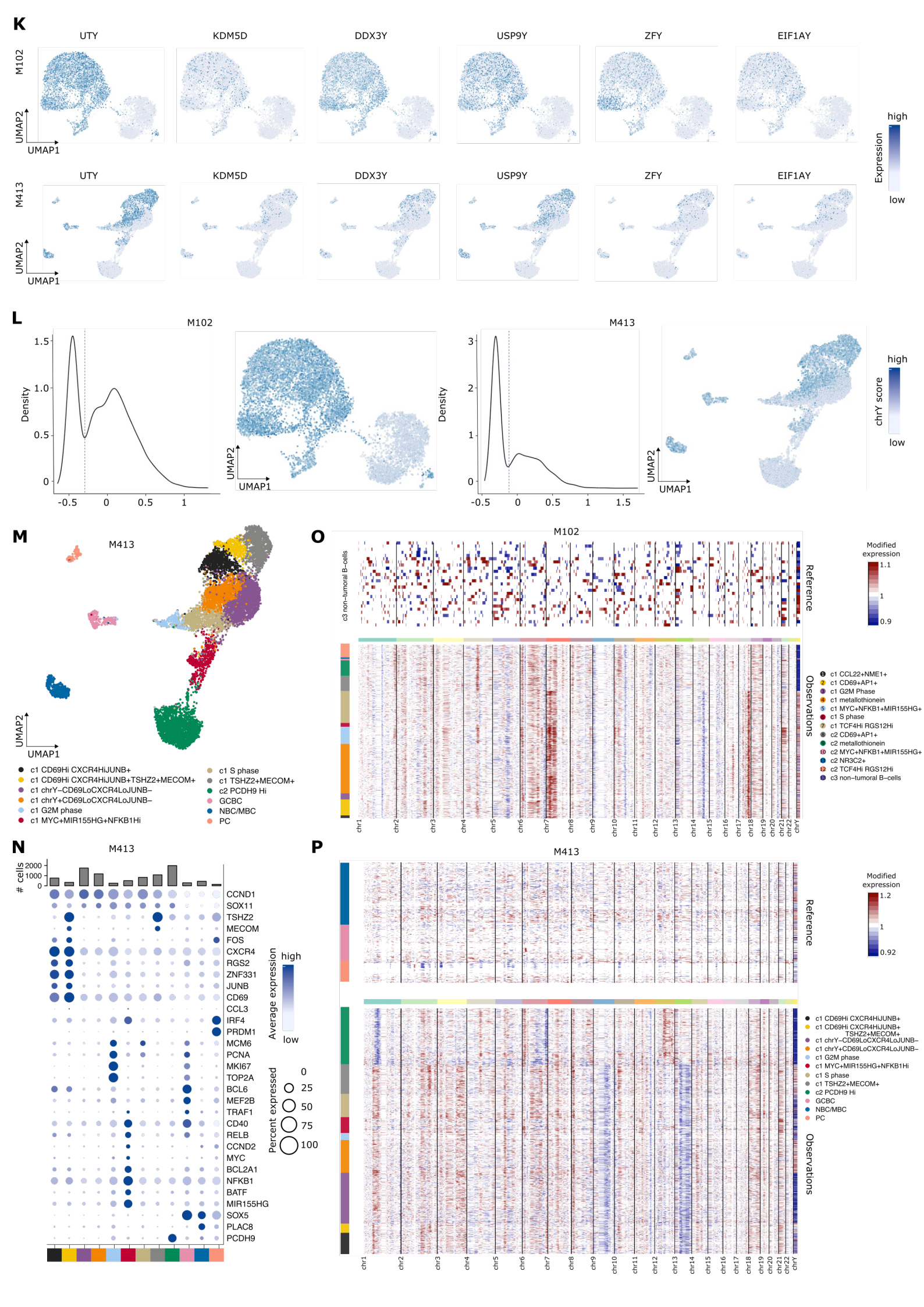
K
UTY
KDM5D
DDX3Y
USP9Y
ZFY
EIF1AY
M102
M413
UMAP2
UMAP1
high
Expression
low
L
M102
M413
Density
chrY score
M
M413
c1 CD69Hi CXCR4HiJUNB+
c1 CD69Hi CXCR4HiJUNB+TSHZ2+MECOM+
c1 chrY−CD69LoCXCR4LoJUNB−
c1 chrY+CD69LoCXCR4LoJUNB−
c1 G2M phase
c1 MYC+MIR155HG+NFKB1Hi
c1 S phase
c1 TSHZ2+MECOM+
c2 PCDH9 Hi
GCBC
NBC/MBC
PC
O
M102
c3 non−tumoral B−cells
Reference
Observations
Modified expression
c1 CCL22+NME1+
c1 CD69+AP1+
c1 G2M Phase
c1 metallothionein
c1 MYC+NFKB1+MIR155HG+
c1 S phase
c1 TCF4Hi RGS12Hi
c2 CD69+AP1+
c2 metallothionein
c2 MYC+NFKB1+MIR155HG+
c2 NR3C2+
c2 TCF4Hi RGS12Hi
c3 non−tumoral B−cells
N
M413
cells
Average expression
Percent expressed
CCND1
SOX11
TSHZ2
MECOM
FOS
CXCR4
RGS2
ZNF331
JUNB
CD69
CCL3
IRF4
PRDM1
MCM6
PCNA
MKI67
TOP2A
BCL6
MEF2B
TRAF1
CD40
RELB
CCND2
MYC
BCL2A1
NFKB1
BATF
MIR155HG
SOX5
PLAC8
PCDH9
P
M413
Reference
Observations
Modified expression